Photomodulation of transmembrane transport and potential by stiff-stilbene based bis(thio)ureas

Wezenberg, S.J.; Chen, L.J.; Bos, J.E.; Feringa, B.L.; Howe, E.N.W.; Wu, X.; ... ; Gale, P.A.

JACS
JOURNAL OF THE AMERICAN CHEMICAL SOCIETY
pubs.acs.org/JACS
Article

Photomodulation of Transmembrane Transport and Potential by Stiff-Stilbene Based Bis(thio)ureas

Sander J. Wezenberg,*[,¶] Li-Jun Chen,[¶] Jasper E. Bos,[¶] Ben L. Feringa, Ethan N. W. Howe, Xin Wu, Maxime A. Siegler, and Philip A. Gale*

Cite This: https://doi.org/10.1021/jacs.1c10034
Read Online

ABSTRACT: Membrane transport proteins fulfill important regulatory functions in biology with a common trait being their ability to respond to stimuli in the environment. Various small-molecule receptors, capable of mediating transmembrane transport, have been successfully developed. However, to confer stimuli-responsiveness on them poses a fundamental challenge. Here we demonstrate photocontrol of transmembrane transport and electric potential using bis(thio)ureas derived from stiff-stilbene. UV−vis and ^{1}H NMR spectroscopy are used to monitor E−Z photoisomerization of these bis(thio)ureas and ^{1}H NMR titrations reveal stronger binding of chloride to the (Z)-form than to the (E)-form. Additional insight into the binding properties is provided by single crystal X-ray crystallographic analysis and DFT geometry optimization. Importantly, the (Z)-isomers are much more active in transmembrane transport than the respective (E)-isomers as shown through various assays. As a result, both membrane transport and depolarization can be modulated upon irradiation, opening up new prospects toward light-based therapeutics as well as physiological and optopharmacological tools for studying anion transport-associated diseases and to stimulate neuronal activity, respectively.

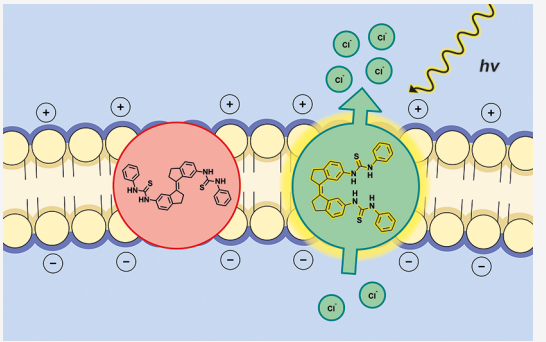

INTRODUCTION

Membrane-embedded transport proteins permit the passage of ions and solutes across the cell's lipid bilayer. They are essential to many important biological functions such as metabolism, ion homeostasis, signal transduction, and regulation of osmotic pressure.[1] A common feature of these proteins is that they exhibit stimuli-responsiveness; i.e. they possess (conformational) switching ability. This responsiveness is, for instance, pivotal in neuronal cells, where chloride-selective gated transporters play a key role in altering membrane potential. Interestingly, light-activated halorhodopsin and anion channel rhodopsins are currently being applied as optogenetic tools to manipulate neuronal activity with high spatiotemporal precision.[2]

Driven by the fact that defects in transmembrane anion transport can cause serious diseases (channelopathies), significant effort has been devoted by the supramolecular chemistry community to develop artificial small-molecule anionophores that, to some extent, imitate and could therefore replace the function of defective proteins.[3] A prime example of such a channelopathy is cystic fibrosis, which is caused by a mutation in the cystic fibrosis transmembrane conductance regulator (CFTR) protein that mediates the translocation of chloride. Hence, synthetic anion transporters hold potential in the study and treatment of diseases associated with dysfunctional transport proteins. Furthermore, some synthetic anion carriers have been shown capable of triggering apoptosis or interfering with autophagy by disrupting cellular ion-homeostasis and therefore have potential as a new class of anticancer agents.[4]

Over the past few years, a large number of artificial anion transporters have been successfully developed,[5] but the integration of stimuli-responsive behavior, as observed in natural systems, remains a tremendous challenge. The most commonly used method to achieve this has been to change the pH value in order to protonate/deprotonate a hydrogen-bond donating anion carrier[6] or to induce conformational changes.[7] Other approaches have included transporters activated by the presence of reducing agents such as GSH found in higher concentrations in tumors than in the surrounding tissue.[8] With respect to light as the stimulus, only a few examples that are either based on azobenzene photoswitches modified with (thio)urea,[9] squaramide,[10] or amide[11] groups or on a photocleavable procarrier[12] are known in the literature. In most cases, however, a more detailed investigation into the

Received: September 22, 2021

https://doi.org/10.1021/jacs.1c10034
J. Am. Chem. Soc. XXXX, XXX, XXX−XXX

mechanism of transport is still to follow. The use of light to control substrate binding and transport has the clear advantage that it can be applied with high spatiotemporal precision and that no chemical waste is generated in the system.[13] In particular, photocontrol of chloride-selective transport would be a highly interesting and promising achievement in the context of developing physiological tools to study diseases associated with defective transport as well as optopharmacological tools to stimulate neuronal activity.

Previously, some of us described the stiff-stilbene based phenyl(thio)ureas **1a**[14] and **2a**[15] shown in Scheme 1. Stiff-stilbene is structurally rigid and is characterized by a high energy barrier to thermal $E-Z$ interconversion and an efficient photoisomerization process, accompanied by a large change in geometry.[16] Consequently, it has proven highly suitable for designing photoresponsive receptors.[17] Compound **1a** could be switched effectively by light between (E)- and (Z)-isomers of which the latter revealed a much larger anion binding affinity, in particular for acetate and dihydrogen phosphate, but also for chloride.[14] Since, among other factors, a partial correlation has been established between binding affinity and chloride transport activity for related receptors,[18] we set out to investigate the transport properties of **1a** and **2a** and their analogues containing electron-withdrawing *p*-trifluoromethyl and *p*-nitro substituents (see Scheme 1). The studies described herein reveal that the (Z)-isomers have much higher activity than the respective (E)-isomers, which allows *in situ* regulation of transmembrane transport by light. Moreover, chloride transport is shown to be selective and light-triggered membrane depolarization, with concomitant generation of a chloride gradient, is shown for the first time using a fully artificial system.

Scheme 1. (a) Photoisomerization of Stiff-Stilbene Based Bis(thio)ureas and (b) Schematic Representation of Photocontrolled Transmembrane Transport

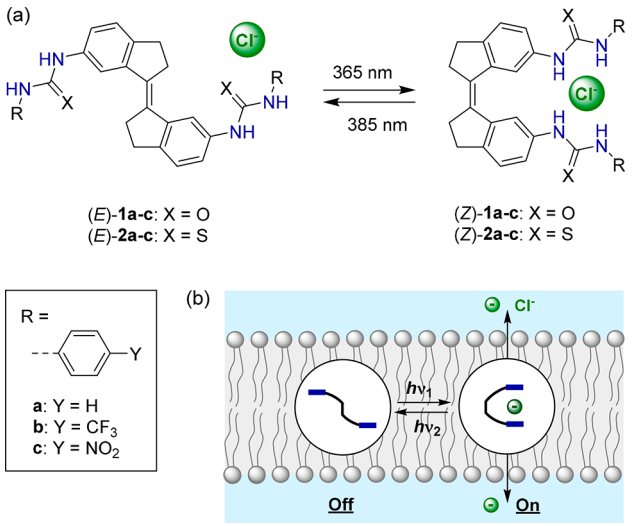

RESULTS AND DISCUSSION

Synthesis and Photoisomerization Behavior. Compounds **1a** and **2a** have been described in earlier work,[14,15] and by using a similar procedure to the one reported; i.e., by reacting either the separately synthesized (E)- or (Z)-stiff-stilbene bis-amine precursor with the corresponding iso(thio)-cyanate, the desired transporters were isolated by filtration and obtained in good yields (67−96%) and purity (see the Supporting Information for synthetic details and characterization).

Their photoswitching properties were investigated in DMSO solution by UV−vis and ^{1}H NMR spectroscopy. The UV−vis absorption spectrum of the *p*-trifluoromethyl-substituted bis-urea (E)-**1b** (Figure 1) was found similar to the one reported for the phenylurea-derivative (E)-**1a**.[14] The thiourea analogues (E)-**2a−b** displayed absorption in the same wavelength region, while the absorption of the *p*-nitrophenyl-substituted bis-(thio)ureas (E)-**1c** and (E)-**2c** extended into the visible light range (see Figures S20−S25). Irradiation of the (E)-isomers with 365 nm light led to a decrease of the absorption maxima around λ = 350 and λ = 365 nm, and for the phenyl- and *p*-trifluoromethylphenyl-substituted compounds, this was accompanied by a small increase in the longer wavelength absorption. These spectral changes are indicative of the unimolecular formation of the respective (Z)-isomers.[14−16] Subsequent irradiation with 385 nm light led to reverse spectral changes, consistent with regeneration of the (E)-isomeric forms. Important to note is that during multiple 365/385 nm irradiation cycles no major signs of degradation were noted for the bis-urea compounds, in contrast to their bis-thiourea counterparts, which proved less fatigue resistant (Figure 1 and Figures S20−S25, insets). Furthermore, in the case of the *p*-nitrophenyl-substituted analogues (E)-**1c** and (E)-**2c**, 365 nm irradiation led to a decrease in overall absorption and the (E)-isomeric forms could not be regenerated by 385 nm irradiation.

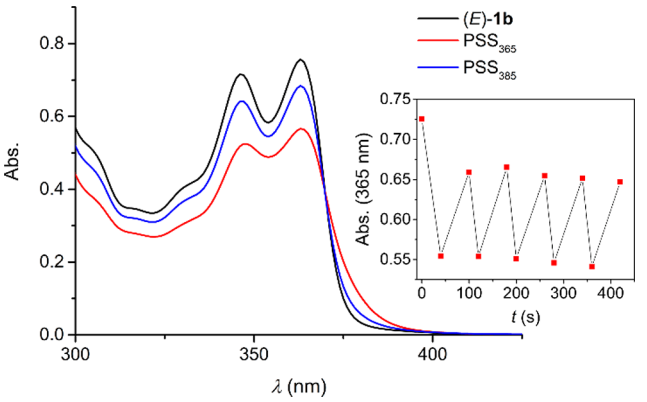

Figure 1. UV−vis spectrum of (E)-**1b** in degassed DMSO (2.5×10^{-4} M) and spectra obtained upon 365 and 385 nm irradiation. The inset shows the absorption change (at 365 nm) upon multiple cycles.

The photostationary state (PSS) ratios were determined by ^{1}H NMR spectroscopy in DMSO-d_6 and are summarized in Table 1. In the ^{1}H NMR spectrum, 365 nm irradiation of the (E)-isomers led to the appearance of a new set of signals with equal chemical shift as observed for the (Z)-isomers synthesized independently (see Figures S26−S29), corroborating $E-Z$ isomerization. Subsequent irradiation with 385 nm light resulted in an increased E/Z integral ratio, demonstrating the reversibility of this photoisomerization process, except for the *p*-nitrophenyl-substituted transporters, which is in line with the observations made by UV−vis spectroscopy (*vide supra*). In general, more (Z)-isomer is formed upon 365 nm irradiation of bis-thioureas **2a−b** than bis-ureas **1a−b**, but on the other hand, the PSS_{385} (E/Z) ratio is the highest for the

https://doi.org/10.1021/jacs.1c10034
J. Am. Chem. Soc. XXXX, XXX, XXX−XXX

Table 1. Photoswitching, Chloride Binding, and Transport Properties of 1a−c and 2a−c

Carrier	$PSS_{365(E/Z)}$	$PSS_{385(E/Z)}$	$K_{1m(E)}$ (M^{-1})[a]	$K_{1m(Z)}$ (M^{-1})[a]	$k_{ini(Z)}$ (% s^{-1})[c]	$k_{ini(E)}$ (% s^{-1})[c]	$F_{(Z/E)}$[d]	$EC_{50(Z)}$ (mol %)[e]	$EC_{50(E)}$ (mol %)[e]	$F'_{(Z/E)}$[g]
1a[14]	49:51	93:7	17	66	0.230	0.034	6.8	0.472	>10[f]	>21.2[h]
1b	65:35	93:7	21	107	0.398	0.036	11.1	0.057	>10[f]	>175.4[h]
1c	n.d.[b]	n.d.[b]	n.d.[b]	103	1.187	0.035	33.9	0.018	>10[f]	>568.8[h]
2a	53:47	83:17	15	93	1.140	0.060	19.1	0.070	2.073	29.7
2b	53:47	74:26	18	125	0.433	0.034	12.8	0.160	>10[f]	>62.5[h]
2c	48:52	48:52	21	102	2.030	0.243	8.4	0.002	0.036	16.3

[a]Microscopic constants ($K_{1m(E)} = K_{11}/2$, $K_{1m(Z)} = K_{11}$) for the first chloride binding event determined by ^{1}H NMR titrations using the tetrabutylammonium salt in DMSO-d_6/0.5% H_2O; errors are estimated to be no more than 15%. [b]Not determined because of poor solubility. [c]Initial rates of chloride transport (k_{ini}) obtained using HPTS assay for each transporter (1 mol %). [d]Factor of enhancement in the Cl^- transport rate between (*Z*)-isomer and (*E*)-isomer ($F_{(Z/E)} = k_{ini(Z)}/k_{ini(E)}$). [e]$EC_{50}$ defined as the effective concentration needed for 50% activity at t = 600 s; values reported in transporter to lipid molar ratio (mol %). [f]Poor transport activity prevented full Hill analysis. [g]Factor of enhancement in the Cl^- transport activity between (*Z*)-isomer and (*E*)-isomer ($F'_{(Z/E)} = EC_{50(E)}/EC_{50(Z)}$). [h]When $EC_{50} > 10$, the EC_{50} value was considered as 10 in factor calculations.

latter. These differences are most likely due to the absorption at the irradiation wavelength not being the same for all compounds.

Chloride Binding Studies. The chloride binding properties of the (*E*)- and (*Z*)-isomers were examined using ^{1}H NMR titrations in DMSO-d_6/0.5% H_2O. In all cases, addition of tetrabutylammonium chloride ($[NBu_4]^+[Cl]^-$) led to gradual downfield shifts of the (thio)urea NH signals as well as relatively small changes in the chemical shifts that belong to the aromatic protons (Figures S30−S38). Since, for the (*E*)-isomers, the relative distance between (thio)urea substituents is too large to bind the chloride ion simultaneously, the titration data were analyzed using a 1:2 binding model (see Scheme S2 for details). HypNMR software[19] was used for the simultaneous fitting of multiple chemical shift changes, and the two (thio)urea binding sites were treated as independent; i.e., the microscopic binding constants for the first and second binding event were assumed to be the same ($K_{1m} = K_{2m}$). This assumption was needed to successfully fit the data because no distinction could be made between ^{1}H NMR chemical shifts of 1:1 and 1:2 complexes throughout the titration. Overall, weak chloride binding was observed with association constants in the range 15−21 M^{-1} (Table 1), similar to other phenyl-(thio)urea transporters.[18]

For the (*Z*)-isomers, Job plot analyses as well as the residual plots obtained by fitting the titration data to both 1:1 and 1:2 binding models using HypNMR (Figures S44−S48) hinted at preferred 1:2 binding, although not conclusively. Single crystals suitable for X-ray structure determination were obtained by slow diffusion of iPr_2O into a solution of (*Z*)-**1c** and 1 equiv of $[NBu_4]^+[Cl]^-$ in $CHCl_3/CCl_4$. The solid-state structure (Figure 2) revealed that the chloride ion can be bound in a 1:1 manner by both *p*-nitrophenylurea substituents simultaneously through four hydrogen bonds with three of the N(H)−Cl^- distances in the range 3.181(2)−3.226(2) Å and the other being 3.354(2) Å. For the NH hydrogen bond donor with the longer N(H)−Cl^- distance, a short contact is observed with the C═O oxygen of a neighboring molecule [N(H)−O distance: 3.327(3) Å] having opposite helical chirality [see Figure S99; note that (*Z*)-**1c** exists in (*P*)- and (*M*)-helical forms].[15] To gain more insight into the preferred binding mode, DFT energy minimization [B3LYP/6-31G++(d,p), IEFPCM DMSO solvation model] of different geometries of (*Z*)-**1a**⊂Cl^- were carried out. These calculations revealed that the structure involving four simultaneous NH−Cl^- hydrogen bonds is about 19 kJ mol^{-1} lower in energy than

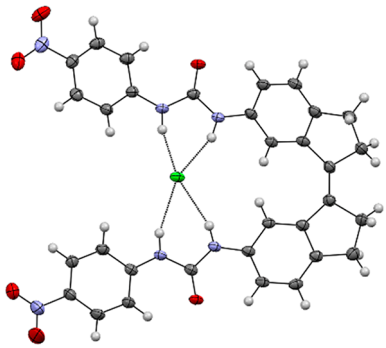

Figure 2. Displacement ellipsoid plot (50% probability level) of (*M*)-(*Z*)-**1c**⊂Cl^- at 110(2) K. The tetrabutylammonium cation has been omitted for clarity.

other possible structures in which the chloride ion is bound by a single urea substituent via two hydrogen bonds (Tables S3−S5). Because of this, the 1:1 geometry with the chloride ion bridging between the (thio)urea groups, as found in the solid state, is expected to prevail in solution. Table 1 shows the association constants obtained when the titration data were fitted using the 1:1 binding model.

Overall, chloride binding to the (*Z*)-isomers was found to be around 5−6 times stronger than to their respective (*E*)-isomers. Transporters with electron-withdrawing *p*-nitro and *p*-trifluoromethyl substituents displayed only slightly higher stability constants,[20] and although their NH protons are more acidic, the bis-thioureas **2a−c** exhibited fairly similar binding strength as the bis-ureas **1a−c**.

Chloride Transport Activity and Selectivity. Following the confirmation that the (*Z*)-isomers show better chloride binding affinity than their respective (*E*)-isomers, a series of membrane transport experiments were conducted in phospholipid vesicles (POPC LUVs with a mean diameter of 200 nm). First, the ion transport properties were examined using 8-hydroxypyrene-1,3,6-trisulfonic acid (HPTS) assays,[21] in which the anion transporter (added to vesicles as DMSO solutions) mediates H^+/Cl^- symport (or Cl^-/OH^- antiport) to dissipate a transmembrane pH gradient (pH 7 inside and pH 8 outside) as monitored by intravesicular pH indicator HPTS. As shown in Figure 3a and Figure S49, the transport activities of the (*Z*)-isomers are all much better than the (*E*)-isomers at the same transporter-to-lipid molar ratio (1 mol %). The initial rates of chloride transport (k_{ini}) obtained are shown in Table 1 and Figure 3b. All the (*E*)-isomers, except (*E*)-**2c**,

https://doi.org/10.1021/jacs.1c10034
J. Am. Chem. Soc. XXXX, XXX, XXX−XXX

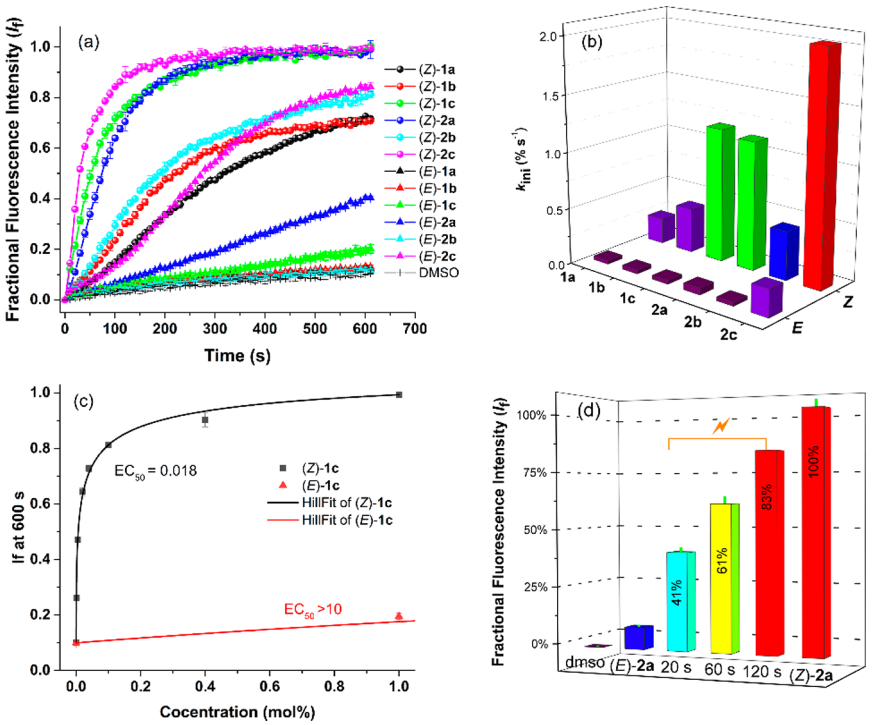

Figure 3. (a) Plots of chloride efflux against time (s) across POPC vesicles facilitated by (*Z*)-isomers (●, 1 mol % to lipid) and (*E*)-isomers (▲, 1 mol % to lipid). (b) Initial rate of chloride transport calculated by exponential or linear fit for each transporter. Detailed experimental conditions are presented in the Supporting Information. (c) Comparison of the concentration−activity curves between (*Z*)-**1c** and (*E*)-**1c**. The solid lines are the fitted curves from Hill equation. (d) Percent transport efficiencies of 365 nm irradiated samples of (*E*)-**2a** plotted relative to the activity of (*Z*)-**2a**.

Table 2. Summary of Cl^- Transport Activity and Cl^- > H^+/OH^- Selectivity of (*Z*)-1a−c and (*Z*)-2a−c (EC_{50} Values Are Shown in Transporter-to-Lipid Molar Ratio (mol %))

Carrier	$EC_{50(BSA)}$ [a]	EC_{50} [b,c]	$EC_{50(BSA\_FCCP)}$ [d]	$EC_{50(FCCP)}$ [e]	F_{FA} [f]	F_s [g]	F'_s [h]
(*Z*)-**1a**	>10[i]	0.472	0.035	0.077	>21.2[j]	>283.7[j]	6.1
(*Z*)-**1b**	>10[i]	0.057	0.091	0.030	>175.4[j]	>110.2[j]	1.9
(*Z*)-**1c**	0.137	0.018	0.141	0.016	7.8	1.0	1.1
(*Z*)-**2a**	1.726	0.070	0.017	0.019	24.7	102.8	3.6
(*Z*)-**2b**	0.703	0.160	0.360	0.155	4.4	2.0	1.0
(*Z*)-**2c**	0.006	0.002	0.007	0.002	2.8	0.8	0.9

[a]EC_{50} in the presence of BSA, showing the total Cl^-/H^+ symport without the presence of fatty acid. [b]EC_{50} in the presence of fatty acid, showing the effect of the natural acceleration of H^+ transport facilitated by fatty acids on the overall transport process. [c]The same data as shown in Table 1. [d]EC_{50} in the presence of BSA and FCCP, showing the maximum Cl^- uniport possible, since without FCCP, H^+/OH^- transport may be rate limiting. [e]EC_{50} in the presence FCCP, showing the maximum Cl^- uniport possible in the presence of fatty acid. [f]Factor of enhancement in the overall rate of Cl^-/H^+ cotransport in the presence of fatty acid, F_{FA} is calculated by dividing the $EC_{50(BSA)}$ by the EC_{50}. F_{FA} > 1 indicates the receptor can assist the flip-flop of fatty acid, increasing pH dissipation. [g]Factor of Cl^- > H^+/OH^- selectivity, F_s is quantified by $EC_{50(BSA)}$ divided by $EC_{50(BSA\_FCCP)}$, F_s > 1 indicates faster Cl^- than H^+/OH^- transport, i.e. Cl^- selective. [h]Factor of Cl^-> H^+/OH^- selectivity retention in the presence of fatty acid, F'_s is calculated by dividing the EC_{50} by the $EC_{50(FCCP)}$, F'_s > 1 indicates Cl^- selective retention in the presence of fatty acid. [i]Poor transport activity prevented full Hill analysis. [j]When EC_{50} > 10, considering the EC_{50} value as 10 in factor calculations.

displayed poor chloride transport activities, whereas the (*Z*)-isomers were at least 7 times more efficient, with the highest enhancement factor of 34 for compound **1c**. The anion transporter potencies of the (*E*)- and (*Z*)-isomers of each anion carrier were further studied using a concentration-dependent Hill analysis to determine the half-maximal effective concentration (EC_{50}, expressed as mol % with respect to lipid concentration) value for H^+/Cl^- symport (or Cl^-/OH^- antiport) processes (Figures S50−S58). As summarized in Table 1, most of the (*E*)-isomers displayed an EC_{50} > 10 indicating poor transport activity, while the analogous (*Z*)-isomers showed significant transport activity with EC_{50} values ranging from 0.472 mol % to 0.002 mol %. The largest difference in activity was observed for compound **1c** (more than 568 times, see Figure 3c and S59).

The comparative ion transport activity of the (*Z*)-isomers provided an activity sequence of **2c** > **1c** > **2a** > **2b** > **1b** > **1a**. In general, bis-thioureas (*Z*)-**2a−c** are better transporters than their urea counterparts (*Z*)-**1a−c**, and electron-withdrawing substituents (CF_3, NO_2) increase the transport activity. This result suggests a role for N−H proton acidity as well as membrane partitioning in the transport activity as comparatively minor stability constant differences were observed in the chloride binding studies (*vide supra*).

The HPTS assay measures the receptor's electroneutral H^+/Cl^- symport (Cl^-/OH^- antiport) ability. In order to further investigate the intrinsic ability of transporters (*Z*)-**1a−c** and

https://doi.org/10.1021/jacs.1c10034
J. Am. Chem. Soc. XXXX, XXX, XXX−XXX

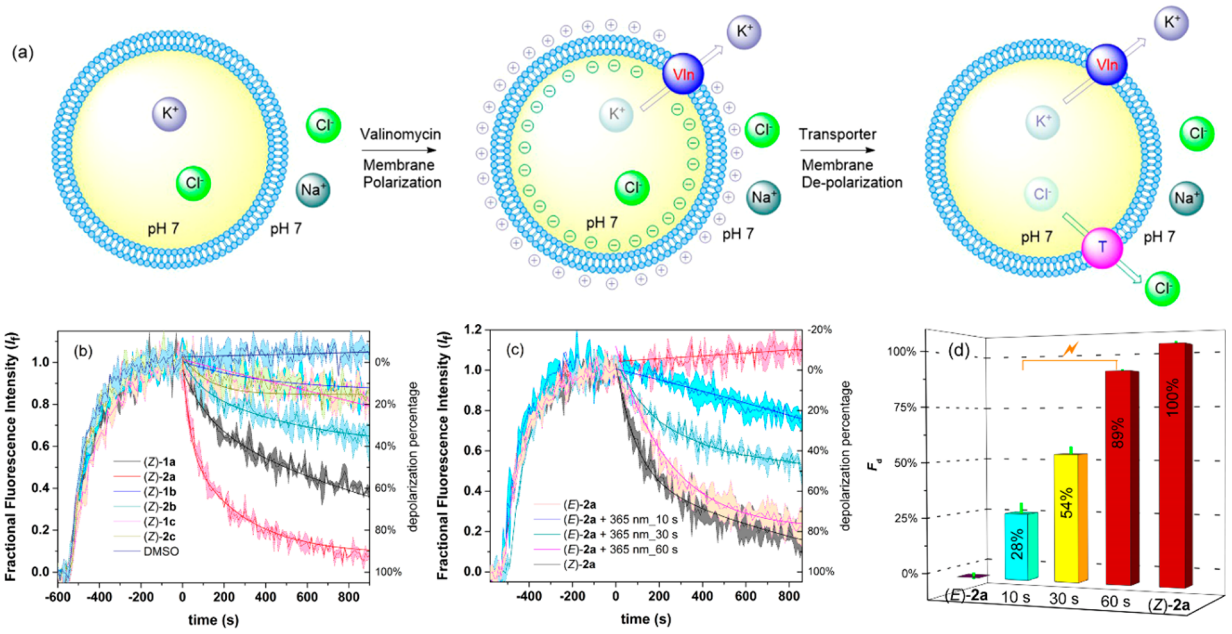

Figure 4. (a) Schematic representation of the Safranin O fluorescence assay. POPC vesicles were loaded with HEPES (10 mM) buffered KCl (100 mM) and suspended in HEPES (10 mM) buffered NaCl (100 mM) with Safranin O and adjusted to pH 7.0. Valinomycin was added to produce polarized liposomes. Once stable emission was observed, 5 μL of a DMSO solution of compound (1 mol % to lipid) was added. (b) The change in emission intensity of safranin O was monitored over time upon addition of (*Z*)-**1a**−**c** and (*Z*)-**2a**−**c** and (c) (*E*)-**2a** before and after 365 nm irradiation. (d) Depolarization efficiencies (%) of irradiated samples of (*E*)-**2a** relative to the activity of (*Z*)-**2a**.

(*Z*)-**2a**−**c** to transport chloride, transport activity was monitored in the presence of carbonyl cyanide-4-(trifluoromethoxy) phenylhydrazone (FCCP, a weak acid protonophore). If the receptor functions as a selective electrogenic Cl^- transporter, addition of FCCP should accelerate the H^+ transport, removing the rate-limiting effect of H^+/OH^- transport.[22] It was reported that some transporters can also facilitate H^+ transport via a fatty acid flip-flop mechanism.[23] Thus, "fatty acid free" vesicles in which BSA was used to sequester fatty acids present in the lipid bilayer were also used to evaluate the ability of the transporters to assist the flip-flop of fatty acids. The concentration-dependent Hill analysis results of these anionophores in the absence and presence of FCCP and fatty acid are presented in Figures S60−S82 and summarized in Table 2. Dividing $EC_{50(BSA)}$ by $EC_{50(BSA\_FCCP)}$ gives F_s values >1 for most receptors, indicating that most of these receptors show chloride transport selectivity under fatty acid free conditions. The unsubstituted compounds (*Z*)-**1a** and (*Z*)-**2a** are extremely selective for Cl^- over H^+ in BSA-treated fatty acid free liposomes, with F_s values of 283 and 102, respectively (Figure S84). As indicated by F_{FA}, quantified by dividing $EC_{50(BSA)}$ by EC_{50}, the transport activity of these anionophores always decreases when fatty acids are removed (Figure S83), indicating that all these receptors can couple via fatty acid flip-flop and enhance the overall rate of H^+/Cl^- symport. The low extent of attenuation observed with the more acidic receptors could suggest a high fatty acid affinity (allowing for the fatty acid flip-flop mechanism even with the traces of fatty acids in equilibrium with BSA) or H^+ transport via a deprotonation mechanism under "fatty acid free" conditions. The chloride transport selectivity retention factor in the presence of fatty acid (F'_s) can be calculated by dividing EC_{50} by $EC_{50(FCCP)}$. Compound (*Z*)-**1a** retained the highest degree of chloride selective transport in the presence of fatty acid with a F'_s = 6.1, while bis-thiourea (*Z*)-**2a** also retained some selectivity in untreated liposomes with a F'_s = 3.6 (Figure S85). The addition of electron-withdrawing groups to the benzene rings decreased the retention of chloride selective transport. The fact that bis-thiourea compound (*Z*)-**2a** could function as an electrogenic Cl^- transporter was also evidenced by the results obtained from cationophore coupled assays.[6,24] Faster Cl^- efflux was observed when coupling with valinomycin (a selective electrogenic K^+ transporter) than with monensin (an electroneutral K^+/H^+ exchanger) (Figure S86), confirming that bis-thiourea (*Z*)-**2a** shows better activity as a Cl^- uniporter than H^+/Cl^- symporter. The findings that the transport mechanism is predominantly electrogenic and (*Z*)-**2a** has a selectivity for $Cl^- > OH^-$ and H^+ was further supported by the osmotic response assay[25] (Figure S87).

Photocontrol of Transmembrane Transport and Potential. Control of transmembrane transport by light was then monitored using an HPTS assay, first. Compound **2a** with both good chloride transport activity and selectivity was selected to examine whether transport could be activated by starting with the (*E*)-isomer and irradiating *in situ*. Sample illumination was achieved using high powered LEDs (see SI for details). As shown above, the transport activity of (*E*)-**2a** (1.0 mol % relative to lipid) is negligible (Figure 3d and Figure S88), but when a vesicle solution containing this (*E*)-isomer was irradiated for 20 s with 365 nm light at the beginning of the experiment, chloride transport was activated with 41% efficiency relative to (*Z*)-**2a**, as a result of *E*−*Z* isomerization. Interestingly, this efficiency was increased up to 83% by prolonging the irradiation time to 120 s to generate more of the active (*Z*)-isomer. Inactivity under comparable conditions with light irradiation for 10 min in the absence of **2a** (Figure S89), indicated that long irradiation times do not destroy the integrity of the lipid bilayer membrane. No switching behavior was observed for a sample of a simple nonphotoresponsive thiourea derivative under comparable conditions with light

https://doi.org/10.1021/jacs.1c10034
J. Am. Chem. Soc. XXXX, XXX, XXX−XXX

irradiation for 10 min (Figure S90), confirming the role of isomerization of **2a** in the photoswitchable transport process.

This light-activated chloride transport was also demonstrated by a cationophore coupled ion selective electrode (ISE) assay (Figures S91−92), in which the transporter-induced chloride efflux coupling with valinomycin or monensin from POPC vesicles containing buffered KCl, suspended in KGlu, was measured in real time using a chloride ISE. Irradiation of (*E*)-**2a** (1.0 mol % relative to lipid) with 365 nm light initiated the transport process, and as expected, it is an electrogenic chloride transport process. The irradiation switched-on transport process could also be demonstrated by a light scattering osmotic response in an osmotic assay (Figure S93) and were consistent with the ISE results. Irradiation of (*Z*)-**2a** (1.0 mol % relative to lipid) with 385 nm light was used to isomerize the transporter within the lipid bilayer membrane, and turn-off the chloride transmembrane transport process (Figure S94). Moreover, reversible switching between the transporting "ON" and "OFF" states was observed an in osmotic assay by *in situ* alternating between 365 and 385 nm light irradiation of (*E*)-**2a** (1.0 mol % relative to lipid) (Figure S95), directly coupling photoisomerization with ion transport. The changes in UV−vis absorption upon 365/385 nm irradiation of **2a** preincorporated into the phospholipid vesicles were similar to those observed in DMSO solution (Figures S23 and S26) illustrating that this activation/deactivation of chloride transport is an effect of *E*−*Z* isomerization.

Among the scarce examples of artificial photoswitchable transporters,[9−11] these compounds represent the first with proven selectivity for Cl^- uniport over H^+/Cl^- symport. An analogy may be drawn with the function of halorhodopsin and anion channel rhodopsin,[2] which use light to stimulate and control the selective flow of chloride across a membrane and thereby are able to hyperpolarize and depolarize cells. This feature allows their use as optogenetic tools to control the activities of neurons. This inspired us to investigate the capacity of our synthetic transporters to modulate membrane potential in polarized liposomes. Hence, POPC-liposomes with internal KCl (100 mM) and external NaCl (100 mM) were prepared to produce a transmembrane K^+ concentration gradient (Figure 4a). The membrane potential of these liposomes was monitored by the probe Safranin O, a membrane potential sensitive fluorescent dye (λ_{em} = 580 nm, λ_{ex} = 520 nm) that can detect the small amount of electrogenic transport possible in vesicular systems.[26] As shown in Figure 4b−c, exogenous addition of the selective K^+ carrier valinomycin led to a significant increase in the emission of Safranin O,[27] because of K^+ efflux established a membrane potential with net negative charge inside the liposomes. Subsequently, upon addition of DMSO solutions of compounds (*Z*)-**1a−c** and (*Z*)-**2a−c** (1 mol %), the fluorescence intensity of Safranin O decreased, indicating depolarization of the lipid bilayer. This process can be attributed to the flow of Cl^- ions out of the polarized liposomes to balance the electrostatic potential established by valinomycin, generating a chloride concentration gradient. Compound (*Z*)-**2a** displayed the highest degree of depolarization with a 98% decrease of fluorescence intensity (Figure 4b). Where all the (*Z*)-isomers showed depolarization activity in liposomes having a transmembrane Cl^- concentration gradient (KCl inside, Na_2SO_4 outside, Figure S96), without this gradient those (*Z*)-isomers with poor Cl^- uniport selectivity (**1b**, **1c**, and **2c**) caused only a slight decrease of the fluorescence (NaCl outside, Figure S97) and thus weak depolarization of vesicles in the case of external NaCl. These results indicate a combined effect of transport activity and Cl^- uniport selectivity in modulating liposomal membrane potential. For transporter **2a**, the degree of liposomal membrane depolarization displayed a nonlinear concentration dependence with an EC_{50} value (effective concentration needed to reach 50% depolarization) of 0.04 mol % (Figure S98). In addition, a nonlinear depolarization activity of (*Z*)-**2a** dependence on the transmembrane potential initialized by valinomycin was observed (Figure S99), indicating that the activity of (*Z*)-**2a** to modulate liposomal membrane potential is voltage dependent. This was also the case when vesicles with internal KCl and an external mixture of K_2SO_4 and Na_2SO_4 were used instead (Figures S100−101).

We then explored the possibility of *in situ* light regulation of liposomal membrane potential. For this purpose, the depolarization activities using samples of (*E*)-**2a** before and after 365 nm irradiation (t = 0, 10, 30, and 60 s) were monitored (Figure 4c−d). As expected, (*E*)-**2a** was inactive prior to irradiation, but the depolarization efficiency (%) with respect to (*Z*)-**2a** was determined as 54% upon irradiating for 30 s and 89% after irradiating the sample for 60 s. A control experiment indicated that long light irradiation did not damage the polarized liposomal membrane (Figure 102). Similar light-regulatory behavior was observed in polarized liposomes having a Cl^- concentration gradient (KCl inside, Na_2SO_4 outside), as judged by the fluorescence intensity decrease of Safranin O (Figure S103). These studies represent the first example of photocontrolled perturbation of membrane potential using synthetic switchable transporters.

CONCLUSIONS

We have presented photoswitchable stiff-stilbene based bis(thio)ureas that display a different binding mode and larger chloride binding affinity in their (*Z*)-form than in their respective (*E*)-form. A series of liposomal membrane transport experiments revealed much higher activity for the (*Z*)-isomers than for the (*E*)-isomers, which allowed *in situ* control over the transport rate by light. Importantly, detailed mechanistic investigation showed that chloride transport mediated by the phenyl(thio)urea-substituted compounds without electron-withdrawing groups is predominantly electrogenic. This feature motivated us to investigate the capacity to perturb membrane potential, for which both transport activity and chloride uniport selectivity proved very important. As a result, light-regulated membrane depolarization and associated generation of a chloride gradient could be achieved for the first time using a fully artificial switchable system. We anticipate that our result will open new perspectives for application of photoswitchable anion transporters in optopharmacology to control neuronal inhibition in an analogous manner to halorhodopsin and rhodopsin,[28] in addition to the development of physiological tools and therapeutics that can be activated and deactivated by light.[29]

ASSOCIATED CONTENT

Supporting Information

This material (PDF) is available free of charge on the ACS Publications Web site: https://pubs.acs.org. The Supporting Information is available free of charge at https://pubs.acs.org/doi/10.1021/jacs.1c10034.

https://doi.org/10.1021/jacs.1c10034
J. Am. Chem. Soc. XXXX, XXX, XXX−XXX

Experimental procedures, characterization of new compounds, ^{1}H NMR and UV−vis studies, DFT-optimization and X-ray analysis (CCDC 2111230), anion transport studies. (PDF)

Accession Codes

CCDC 2111230 contains the supplementary crystallographic data for this paper. These data can be obtained free of charge via www.ccdc.cam.ac.uk/data_request/cif, or by emailing data_request@ccdc.cam.ac.uk, or by contacting The Cambridge Crystallographic Data Centre, 12 Union Road, Cambridge CB2 1EZ, UK; fax: +44 1223 336033.

AUTHOR INFORMATION

Corresponding Authors

Sander J. Wezenberg − *Leiden Institute of Chemistry, Leiden University, 2333 CC Leiden, The Netherlands; Stratingh Institute for Chemistry, University of Groningen, 9747 AG Groningen, The Netherlands;* orcid.org/0000-0001-9192-3393; Email: s.j.wezenberg@lic.leidenuniv.nl

Philip A. Gale − *School of Chemistry, The University of Sydney, Sydney, NSW 2006, Australia; The University of Sydney Nano Institute (SydneyNano), The University of Sydney, Sydney, NSW 2006, Australia*; Email: philip.gale@sydney.edu.au

Authors

Li-Jun Chen − *School of Chemistry, The University of Sydney, Sydney, NSW 2006, Australia*

Jasper E. Bos − *Leiden Institute of Chemistry, Leiden University, 2333 CC Leiden, The Netherlands*

Ben L. Feringa − *Stratingh Institute for Chemistry, University of Groningen, 9747 AG Groningen, The Netherlands;* orcid.org/0000-0003-0588-8435

Ethan N. W. Howe − *School of Chemistry, The University of Sydney, Sydney, NSW 2006, Australia;* Present Address: Present address: GlaxoSmithKline, GSK Jurong, 1 Pioneer Sector1, Singapore 628413

Xin Wu − *School of Chemistry, The University of Sydney, Sydney, NSW 2006, Australia;* orcid.org/0000-0002-7715-8784

Maxime A. Siegler − *Department of Chemistry, Johns Hopkins University, Baltimore, Maryland 21218, United States;* orcid.org/0000-0003-4165-7810

Complete contact information is available at: https://pubs.acs.org/10.1021/jacs.1c10034

Author Contributions

¶S.J.W., L.-J.C. and J.E.B. contributed equally to this work.

Notes

The authors declare no competing financial interest.

ACKNOWLEDGMENTS

We gratefully acknowledge financial support from the European Research Council (Starting Grant no. 802830 to S.J.W. and Advanced Grant no. 694345 to B.L.F.) and The Netherlands Organization for Scientific Research (NWO-ENW, Vidi Grant no. VI.Vidi.192.049 to S.J.W.). We thank Dr. Karthick B. Sai Sankar Gupta and Alfons Lefeber for help with NMR experiments. L.-J.C., X.W. and P.A.G. acknowledge and pay respect to the Gadigal people of the Eora Nation, the traditional owners of the land on which we research, teach, and collaborate at the University of Sydney. P.A.G. thanks the University of Sydney and the Australian Research Council (DP200100453) for funding.

REFERENCES

(1) Cooper, G. M. *The Cell: A Molecular Approach*, 8th ed.; Oxford University Press: 2019; pp 45−80.

(2) Schobert, B.; Lanyi, J. K. Halorhodopsin is a light-driven chloride pump. *J. Biol. Chem.* **1982**, *257*, 10306−10313. (b) Engelhard, C.; Chizhov, I.; Siebert, F.; Engelhard, M. Microbial halorhodopsins: light-driven chloride pumps. *Chem. Rev.* **2018**, *118*, 10629−10645.

(3) (a) Li, H.; Valkenier, H.; Thorne, A. G.; Dias, C. M.; Cooper, J. A.; Kieffer, M.; Busschaert, N.; Gale, P. A.; Sheppard, D. N.; Davis, A. P. Anion carriers as potential treatments for cystic fibrosis: transport in cystic fibrosis cells, and additivity to channel-targeting drugs. *Chem. Sci.* **2019**, *10*, 9663−9672. (b) Davis, J. T.; Gale, P. A.; Quesada, R. Advances in anion transport and supramolecular medicinal chemistry. *Chem. Soc. Rev.* **2020**, *49*, 6056−6086.

(4) (a) Ko, S.-K.; Kim, S. K.; Share, A.; Lynch, V. M.; Park, J.; Namkung, W.; Van Rossom, W.; Busschaert, N.; Gale, P. A.; Sessler, J. L.; Shin, I. Synthetic ion transporters can induce apoptosis by facilitating chloride anion transport into cells. *Nat. Chem.* **2014**, *6*, 885−892. (b) Rodilla, L.; Korrodi-Gregório, A. M.; Hernando, E.; Manuel-Manresa, P.; Quesada, R.; Pérez-Tomás, R.; Soto-Cerrato, V. Synthetic tambjamine analogues induce mitochondrial swelling and lysosomal dysfunction leading to autophagy blockade and necrotic cell death in lung cancer. *Biochem. Pharmacol.* **2017**, *126*, 23−33. (c) Manuel-Manresa, P.; Korrodi-Gregório, L.; Hernando, E.; Villanueva, A.; Martínez-García, D.; Rodilla, A. M.; Ramos, R.; Fardilha, M.; Moya, J.; Quesada, R.; Soto-Cerrato, V.; Pérez-Tomás, R. Novel Indole-based Tambjamine-Analogues Induce Apoptotic Lung Cancer Cell Death through p38 Mitogen-Activated Protein Kinase Activation. *Mol. Cancer Ther.* **2017**, *16*, 1224−1235. (d) Zhang, S.; Wang, Y.; Xie, W.; Howe, E. N. W.; Busschaert, N.; Sauvat, A.; Leduc, M.; Gomes-da-Silva, L. C.; Chen, G.; Martins, I.; Deng, X.; Maiuri, L.; Kepp, O.; Soussi, T.; Gale, P. A.; Zamzami, N.; Kroemer, G. Squaramide-based synthetic chloride transporters activate TFEB but block autophagic flux. *Cell Death & Disease* **2019**, *10*, 242. (e) Park, S.-H.; Park, S.-H.; Howe, E. N. W.; Hyun, J. Y.; Chen, L.-J.; Hwang, I. C.; Vargas-Zuñiga, G.; Busschaert, N.; Gale, P. A.; Sessler, J. L.; Shin, I. Determinants of Ion-Transporter Cancer Cell Death. *Chem.* **2019**, *5*, 2079−2098.

(5) (a) Busschaert, N.; Caltagirone, C.; Van Rossom, W.; Gale, P. A. Applications of Supramolecular Anion Recognition. *Chem. Rev.* **2015**, *115*, 8038−8155. (b) Chen, L.; Berry, S. N.; Wu, X.; Howe, E. N. W.; Gale, P. A. Advances in Anion Receptor Chemistry. *Chem.* **2020**, *6*, 61−141. (c) Wu, X.; Gilchrist, A. M.; Gale, P. A. Prospects and Challenges in Anion Recognition and Transport. *Chem.* **2020**, *6*, 1296−1309.

(6) (a) Busschaert, N.; Elmes, R. B. P.; Czech, D.; Wu, X.; Kirby, I. L.; Peck, E. M.; Hendzel, K. D.; Shaw, S. K.; Chan, B.; Smith, B. D.; Jolliffe, K. A.; Gale, P. A. Thiosquaramides: pH switchable anion transporters. *Chem. Sci.* **2014**, *5*, 3617−1326. (b) Roy, A.; Saha, D.; Mandal, P. S.; Mukherjee, A.; Talukdar, P. pH-gated Chloride Transport by a Triazine-Based Tripodal Semicage. *Chem. - Eur. J.* **2017**, *23*, 1241−1247. (c) Saha, A.; Akhtar, N.; Kumar, V.; Kumar, S.; Srivastava, H. K.; Kumar, S.; Manna, D. pH-regulated anion transport activities of bis(iminourea) derivatives across the cell and vesicle membrane. *Org. Biomol. Chem.* **2019**, *17*, 5779−5788. (d) Tapia, L.; Pérez, Y.; Bolte, M.; Casas, J.; Solá, J.; Quesada, R.; Alfonso, I. pH-Dependent Chloride Transport by Pseudopeptidic Cages for the Selective Killing of Cancer Cells in Acidic Microenvironments. *Angew. Chem., Int. Ed.* **2019**, *58*, 12465−12468.

(7) (a) Santacroce, P. V.; Davis, J. T.; Light, M. E.; Gale, P. A.; Iglesias-Sánchez, J. C.; Prados, P.; Quesada, R. Conformational Control of Transmembrane Cl^- Transport. *J. Am. Chem. Soc.* **2007**, *129*, 1886−1887. (b) Howe, E. N. W.; Busschaert, N.; Wu, X.; Berry, S. N.; Ho, J.; Light, M. E.; Czech, D. D.; Klein, H. A.; Kitchen, J. A.; Gale, P. A. pH-Regulated Nonelectrogenic Anion Transport by Phenylthiosemicarbazones. *J. Am. Chem. Soc.* **2016**, *138*, 8301−8308.

(8) (a) Akhtar, N.; Pradhan, N.; Saha, A.; Kumar, V.; Biswas, O.; Dey, S.; Shah, M.; Kumar, S.; Manna, D. Tuning the solubility of ionophores: glutathione-mediated transport of chloride ions across hydrophobic membranes. *Chem. Commun.* **2019**, *55*, 8482−8485. (b) Fares, M.; Wu, X.; Ramesh, D.; Lewis, W.; Keller, P. A.; Howe, E. N. W.; Pérez-Tomás, R.; Gale, P. A. Stimuli-responsive cycloaurated "OFF-ON" Switchable Anion Transporters. *Angew. Chem., Int. Ed.* **2020**, *59*, 17614−17621. (c) Malla, J. A.; Umesh, R. M.; Yousf, S.; Mane, S.; Sharma, S.; Lahiri, M.; Talukdar, P. A Glutathione Activatable Ion Channel Induces Apoptosis in Cancer Cells by Depleting Intracellular Glutathione Levels. *Angew. Chem., Int. Ed.* **2020**, *59*, 7944−7952. (d) Park, G.; Gabbaï, F. P. Redox-controlled chalcogen and pnictogen bonding: the case of a sulfonium/stibonium dication as a preanionophore for chloride anion transport. *Chem. Sci.* **2020**, *11*, 10107−10112.

(9) Choi, Y. R.; Kim, G. C.; Jeon, H.-G.; Park, J.; Namkung, W.; Jeong, K.-S. Azobenzene-based chloride transporters with light-controllable activities. *Chem. Commun.* **2014**, *50*, 15305−15308.

(10) (a) Kerckhoffs, A.; Bo, Z.; Penty, S. E.; Duarte, F.; Langton, M. J. Red-shifted tetra-*ortho*-halo-azobenzenes for photo-regulated transmembrane anion transport. *Org. Biomol. Chem.* **2021**, *19*, 9058−9067. (b) Kerckhoffs, A.; Langton, M. J. Reversible photo-control over transmembrane anion transport using visible-light responsive supramolecular carriers. *Chem. Sci.* **2020**, *11*, 6325−6331.

(11) Ahmad, M.; Metya, S.; Das, A.; Talukdar, P. A Sandwich Azobenzene-Diamide Dimer for Photoregulated Chloride Transport. *Chem. - Eur. J.* **2020**, *26*, 8703−8708.

(12) Salunke, S. B.; Malla, J. A.; Talukdar, P. Phototriggered Release of a Transmembrane Chloride Carrier form an *o*-Nitrobenzyl-Linked Procarrier. *Angew. Chem., Int. Ed.* **2019**, *58*, 5354−5358.

(13) (a) Shinkai, S.; Manabe, O. Photocontrol of Ion Extraction and Ion Transport by Photofunctional Crown Ethers. *Top. Curr. Chem.* **1984**, *121*, 67−104. (b) Lee, S.; Flood, A. H. Photoresponsive Receptors for Binding and Releasing Anions. *J. Phys. Org. Chem.* **2013**, *26*, 79−86. (c) Qu, D.-H.; Wang, Q.-C.; Zhang, Q.-W.; Ma, X.; Tian, H. Photoresponsive Host-Guest Functional Systems. *Chem. Rev.* **2015**, *115*, 7543−7588. (d) García-Lopez, V.; Chen, F.; Nilewski, L. G.; Duret, G.; Aliyan, A.; Kolomeisky, A.; Robinson, J. T.; Wang, G.; Pal, R.; Tour, J. A. Molecular machines open cell membranes. *Nature* **2017**, *548*, 567−572. (e) Langton, M. J. Engineering of stimuli-responsive lipid-bilayer membranes using supramolecular systems. *Nat. Rev. Chem.* **2021**, *5*, 46−61. (f) Wang, C.; Wang, S.; Yang, H.; Xiang, Y.; Wang, X.; Bao, C.; Zhu, L.; Tian, H.; Qu, D.-H. A Light-Operated Molecular Cable Car for Gated Ion Transport. *Angew. Chem., Int. Ed.* **2021**, *60*, 14836−14840. (g) Wang, W.-Z.; Huang, L.-B.; Zheng, S.-P.; Moulin, E.; Gavat, O.; Barboiu, M.; Giuseppone, N. Light-Driven Molecular Motors Boost the Selective Transport of Alkali Metal Ions through Phospholipid Bilayers. *J. Am. Chem. Soc.* **2021**, *143*, 15653−15660.

(14) Wezenberg, S. J.; Feringa, B. L. Photocontrol of Anion Binding Affinity to a Bis-urea Receptor Derived from Stiff-Stilbene. *Org. Lett.* **2017**, *19*, 324−327.

(15) Wezenberg, S. J.; Feringa, B. L. Supramolecularly directed rotary motion in a photoresponsive receptor. *Nat. Commun.* **2018**, *9*, 1984.

(16) (a) Waldeck, D. H. Photoisomerization Dynamics of Stilbene. *Chem. Rev.* **1991**, *91*, 415−436. (b) Villarón, D.; Wezenberg, S. J. Stiff-Stilbene Photoswitches: From Fundamental Studies to Emergent Applications. *Angew. Chem., Int. Ed.* **2020**, *59*, 13192−13202.

(17) (a) Xu, J.-F.; Chen, Y.-Z.; Whu, L.-Z.; Tung, C.-H.; Yang, Q.-Z. Synthesis of a Photoresponsive Cryptand and Its Complexations with Paraquat and 2,7-Diazapyrenium. *Org. Lett.* **2014**, *16*, 684−687. (b) Wang, Y.; Tian, Y.; Chen, Y.-Z.; Niu, L. Y.; Wu, L.-Z.; Tung, C.-H.; Yang, Q.-Z.; Boulatov, R. A light-driven molecular machine based on stiff stilbene. *Chem. Commun.* **2018**, *54*, 7991−7994. (c) MacDonald, T. S. C.; Feringa, B. L.; Price, W. S.; Wezenberg, S. J.; Beves, J. E. Controlled Diffusion of Photoswitchable Receptors by Binding Anti-electrostatic Hydrogen-Bonded Phosphate Oligomers. *J. Am. Chem. Soc.* **2020**, *142*, 20014−20020. (d) Villarón, D.; Siegler, M. A.; Wezenberg, S. J. A photoswitchable strapped calix[4]pyrrole receptor: highly effective chloride binding and release. *Chem. Sci.* **2021**, *12*, 3188−3193.

(18) Busschaert, N.; Kirby, I. L.; Young, S.; Coles, S. J.; Horton, P. M.; Light, M. E.; Gale, P. A. Squaramides as Potent Transmembrane Anion Transporters. *Angew. Chem., Int. Ed.* **2012**, *51*, 4426−4430.

(19) Frassineti, C.; Ghelli, S.; Gans, P.; Sabatini, A.; Moruzzi, M. S.; Vacca, A. Nuclear Magnetic Resonance as a Tool for Determining Protonation Constants of Natural Polyprotic Bases in Solution. *Anal. Biochem.* **1995**, *231*, 374−382.

(20) Brooks, S. J.; Edwards, P. R.; Gale, P. A.; Light, M. E. Carboxylate complexation by a family of easy-to-make *ortho*-phenylenediamine based bis-ureas: studies in solution and the solid state. *New J. Chem.* **2006**, *30*, 65−70.

(21) Wu, X.; Howe, E. N. W.; Gale, P. A. Supramolecular Transmembrane Anion Transport: New Assays and Insights. *Acc. Chem. Res.* **2018**, *51*, 1870−1879.

(22) Wu, X.; Judd, L. W.; Howe, E. N. W.; Withecombe, A. M.; Soto-Cerrato, V.; Li, H.; Busschaert, N.; Valkenier, H.; Pérez-Tomás, R.; Sheppard, D. N.; Jiang, Y.-B.; Davis, A. P.; Gale, P. A. Nonprotonophoric Electrogenic Cl^- Transport Mediated by Valinomycin-like Carriers. *Chem.* **2016**, *1*, 127−146.

(23) (a) Wu, X.; Gale, P. A. Small-Molecule Uncoupling Protein Mimics: Synthetic Anion Receptors as Fatty Acid-Activated Proton Transporters. *J. Am. Chem. Soc.* **2016**, *138*, 16508−16514. (b) Howe, E. N. W.; Gale, P. A. Fatty Acid Fueled Transmembrane Chloride Transport. *J. Am. Chem. Soc.* **2019**, *141*, 10654−10660.

(24) Jowett, L. A.; Howe, E. N. W.; Wu, X.; Busschaert, N.; Gale, P. A. New Insights into the Anion Transport Selectivity and Mechanism of Tren-based Tris-(thio)ureas. *Chem. - Eur. J.* **2018**, *24*, 10475−10487.

(25) Clarke, H. J.; Howe, E. N. W.; Wu, X.; Sommer, F.; Yano, M.; Light, M. E.; Kubik, S.; Gale, P. A. Transmembrane Fluoride Transport: Direct Measurement and Selectivity Studies. *J. Am. Chem. Soc.* **2016**, *138*, 16515−16522.

(26) Woolley, G. A.; Deber, C. M. A lipid vesicle system for probing voltage-dependent peptide-lipid interactions: application to alamethicin channel formation. *Biopolymers* **1989**, *28*, 267−272.

(27) Li, X.; Shen, B.; Yao, X. Q.; Yang, D. Synthetic chloride channel regulates cell membrane potentials and voltage-gated calcium channels. *J. Am. Chem. Soc.* **2009**, *131*, 13676−13680.

(28) Fenno, L.; Yizhar, O.; Deisseroth, K. The development and application of optogenetics. *Annu. Rev. Neurosci.* **2011**, *34*, 389−412.

(29) (a) Velema, W. A.; Szymanski, W.; Feringa, B. L. Photopharmacology: Beyond Proof of Principle. *J. Am. Chem. Soc.* **2014**, *136*, 2178−2191. (b) Broichhagen, J.; Frank, J. A.; Trauner, D. A Roadmap to Success in Photopharmacology. *Acc. Chem. Res.* **2015**, *48*, 1947−1960. (c) Welleman, I. M.; Hoorens, M. W. H.; Feringa, B. L.; Boersma, H. H.; Szymañski, W. Photoresponsive molecular tools for emerging applications of light in medicine. *Chem. Sci.* **2020**, *11*, 11672−11691.

https://doi.org/10.1021/jacs.1c10034
J. Am. Chem. Soc. XXXX, XXX, XXX−XXX